Core intrinsic toroidal rotation mechanisms tested against ASDEX Upgrade observations

W A Hornsby[1], C Angioni[1], E Fable[1], P Manas[1], R McDermott[1], A G Peeters[2] and the ASDEX Upgrade Team

[1] Max-Planck-Institut für Plasmaphysik, Boltzmannstrasse 2, D-85748
[2] Theoretical Physics V, Dept. of Physics, Universität Bayreuth, Bayreuth, Germany, D-95447

E-mail: william.hornsby@ipp.mpg.de

Toroidal momentum transport is closely linked to symmetry breaking in the direction along the strong background magnetic field. At lowest order (in expansion parameter $\rho_* = \rho_i/R_0$) and in a non-rotating state the gyro-kinetic equation used to describe turbulent fluctuations, has a series of symmetries that prohibits momentum transport [1]. Toroidal momentum transport is intrinsically linked to mechanisms that break these symmetries. Mechanisms of residual stress generation that can be described in flux-tube geometry include, amongst others, up-down flux surface asymmetry, higher order corrections to the parallel derivatives and the influence of background neoclassical and diamagnetic flows and have been shown to be small by analysing a large database [2] of ASDEX Upgrade L-mode plasmas [3, 4].

A number of symmetry breaking mechanisms are reliant on the radial variation of equilibrium and geometric quantities. These include profile shearing which is linked to the tilting of mode structure by the radial variation of equilibrium. These can not be captured in a flux tube, local simulation and hence require global gyro-kinetic simulations to evaluate their amplitudes.

Here we concentrate on the high density phase (t = 2.8s) of a L-mode Ohmic AUG shot (# 27000), which features a density ramp. Here, the predominant linear mode is the ITG. The radial ion logarithmic temperature gradient, logarithmic density gradient, safety factor (q) and magnetic shear ($\hat{s}$) profiles for this shot are shown in right hand panels of Fig. 1. Global GKW [5] simulations are run with kinetic electrons and hydrogen ions ($m_i/m_e = 1860$) over the toroidal wave number range $k_\zeta \rho_i \leq 1.32$. The simulations are run electro-magnetically with a small value of the electron β ($3{\cdot}10^{-4}$) for numerical stability reasons. The radial grid spacing is chosen so that 3 grid points per gyro-radius resolution ($\Delta r/\rho_i = \Delta\psi/(N_x\rho_*) \sim 0.31$) is maintained. The radial domain spans $0.01 \leq \psi = r/R_0 \leq 0.245$ which corresponds to $0.03 \leq r/a \leq 0.8$ where a is the minor radius.

The final flow state in a global turbulence simulation is determined when the diffusive momentum flux generated by the non-linearly generated flow gradients balances point-by-point the residual stress. The top left panel Fig. 1 shows the radial profiles of the parallel flow as calculated by GKW in black (shifted in magnitude to match the flow at $r/a = 0.24$). It shows a dipole like structure which is enforced by the no-slip boundary conditions and the conservation of momentum. It can be seen that in the centre of the domain the simulated flow profile and gradient agree extremely well with the experiment. It should be noted that in this case in the previous study using

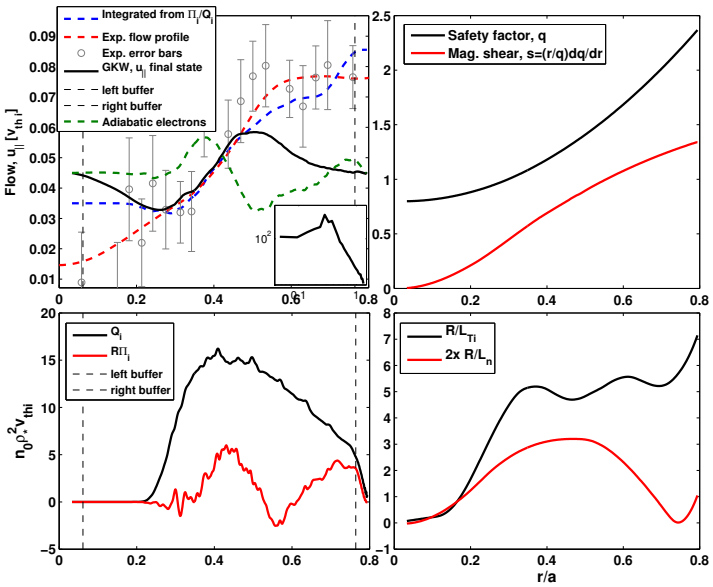

Figure 1. (top left) The radial profiles of the turbulence generated flow profile. In inlay is the time and spatially averaged turbulent spectrum in the electrostatic fluctuations. (top right) The radial profiles of the safety factor (black) and magnetic shear ($\hat{s} = (r/q)\partial q/\partial r$,grey). (lower left) The time averaged radial heat (black) and momentum (red) flux just after the linear overshoot of the simulation. The vertical dashed lines denote the buffer regions where the turbulence is damped away near the boundaries. (lower right) The radial profiles of the ion temperature (black) and density (red) scale lengths for Shot number # 27000, $t = 2.80s$.

flux-tube simulations outlined in the previous chapters, the sum of all the gradients was very small and as such global mechanisms would be expected to make up most the flow gradient at mid radius. Also plotted is (in red) the fitted experimental intrinsic flow profile and the corresponding raw data points and error bars measured by charge exchange recombination spectroscopy (CXRS).

A damping region is used at the edge of the computational domain to minimise the effects of the boundary conditions and these areas are denoted by vertical dashed lines. The flow, and its gradient, are free in the centre of the domain to attain the value as determined by the turbulence. The Dirichelet boundary conditions are restrictive on the flow profile, setting the flow to zero at the boundaries, but their effect on the turbulence, and the turbulent momentum and heat fluxes is smaller apart from inside the imposed edge buffers. Assuming that the total toroidal momentum flux is made up of only the diffusive (ion viscous) component and a residual stress, in steady state, these components would balance each other to produce a flow gradient of the form $u' = -\frac{\Pi_i}{Q_i}\frac{R}{L_{T_i}}\frac{1}{P_r}\frac{v_{thi}}{R}$. The residual flow profile can be calculated from early time, before the zonal and toroidal flows are established in the simulation which have a large effect on the momentum flux. This residual stress profile can then be integrated to produce a flow profile which is plotted as a blue dashed line in Fig. 1. This shows excellent agreement with the experimental flow profile, being largely within the error bars of the measurement. Here the Prandtl number ($Pr = 0.63$) used is calculated from a quasi-linear flux-tube simulation at mid-radius using nominal parameters. The flow profile when using an adiabatic electron model (green dashed line in figure) is reversed with respect to the kinetic electron case.

Density evolution and its effect on profile shearing

To maintain background temperature profiles, global simulations utilise a Krook style operator of the form,

$$\left.\frac{\partial f(v_\parallel,\mu)}{\partial t}\right|_K = -\gamma_K\left[\frac{1}{2}[f(v_\parallel,\mu)+f(-v_\parallel,\mu)]-\tilde{n}F_M(v_\parallel,\mu)\right], \qquad (1)$$

where f is the perturbed distribution function, F_M is the local Maxwellian and $\tilde{n}$ is the local perturbed density. A value of $\gamma_K = 0.028$ is used for the rate coefficient. This form of operator, does not act to maintain the density profile. In simulations with adiabatic electrons this means that the density and temperature profiles stay very close (within 1%) of the equilibrium profile since the particle flux is zero. However, when kinetic electrons are used the density profile, due to non-zero particle fluxes, is allowed to evolve (Examples are shown in the top right panel of Fig. 2). What is observed is a direct correlation between the perturbation of the density profile and the parallel flow gradients seen in the simulation (lower panel). As the profile relaxes, increasing the curvature of the density profile, the local flow gradient increases accordingly. This corresponds to an increased residual stress due to an increase in profile shearing (Remembering that the residual stress due to profile shearing, $\Pi_{res} = \Pi_{res}(n_e, n_e', n_e'', T_i, T_i', T_i''...)$). The density profile evolution also goes to explain why hollow profiles are always seen in kinetic electron simulations, even when peaked or flat flow profiles are expected since the curvature of the profile due to its relaxation is always seen to be in the same direction.

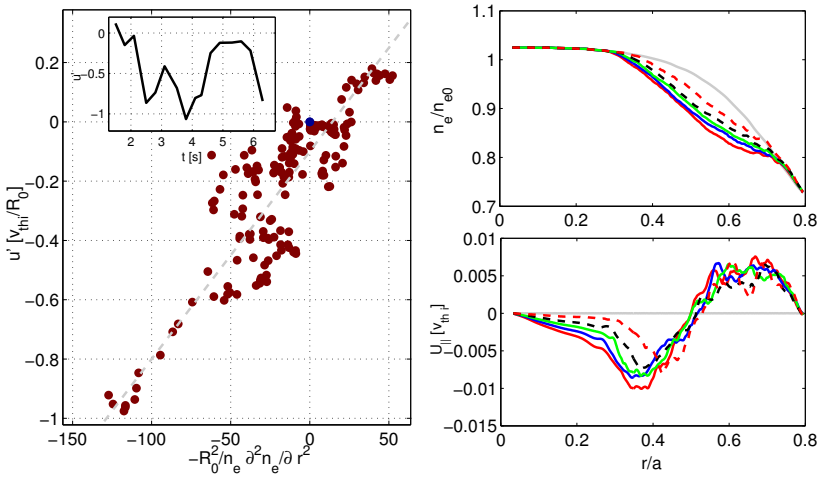

Figure 2. (Left) The flow gradient, u' as function of the second derivative of the time averaged and spatially averaged density profile in global turbulence simulations at $\rho_* = 0.0015$. In inlay the u' time trace at $\rho_T = 0.5$ for Shot # 27000. (Right) Examples of total density profile (top) and flow profile (bottom) at a series of time slices.

By slicing the radial domain into 4 different zones then also the time evolution of the flow gradient and the density profile into time windows and using this to sample the data, we are able to plot the flow gradient as a function of normalised second derivative of the density ($-R_0^2/n_e\frac{\partial^2 n_e}{\partial r^2} = \alpha$). This is plotted for three simulations with kinetic electrons based around the above simulation in Fig. 2. From a linear fit to this data we can estimate that, due to density profile curvature, and via profile

shearing the residual stress can give a flow gradient of,

$$u' \sim -0.008 \frac{R_0^2}{n_e} \frac{\partial^2 n_e}{\partial r^2} = 0.008\alpha. \quad (2)$$

In Fig. 2, we present a time trace from Shot number # 27000 at $\rho_T = 0.5$. It is evident that during a single shot, at a single radial location, u' may vary by a factor of 0.8. Using the above estimate this would require a variation of density profile curvature of $\alpha \sim 100$. We see from the reflectometry profile data (See for example Figs. 10 and 11 in Ref.[3]) that variations of this magnitude, unlike the neoclassical background flows, are consistent with the measured profiles on AUG and that, variations of this amplitude are seen within a shot and can go towards explaining the observed flow changes.

The role of the density profile on the generation of residual stress is underlined by taking the late-time, relaxed, density profile from a kinetic electron simulation and using it as the equilibrium profile with adiabatic electrons. Keeping all other parameters the same (same simulation that gives the green dashed curve in Fig. 1) we see that the residual stress, and the corresponding flow profile are reversed with respect to the unperturbed density profiles.

Conclusions

The effect of various mechanisms of toroidal momentum transport in the ASDEX Upgrade tokamak was studied using gyro-kinetic turbulence simulations. The combined effects of neoclassical flows, E×B velocity flow shear, Coriolis pinch, up-down asymmetry in the equilibrium and higher order corrections to the parallel derivatives is insufficient to explain the flow gradients that are measured.

Global simulations of a selected subset show good agreement in some cases. However, it is seen that with kinetic electrons, simulations always give steep hollow profiles even when the experiment shows flat or peaked profiles. Time evolution of the density profile due to finite particle fluxes in simulations go towards explaining this and also give a way of quantifying the effects of curvature in the density profile on profile shearing as a residual stress mechanism. Using this it is shown that variation of curvature can strongly vary the residual stress. Variations in the density profile curvature are consistent in magnitude with the levels found in density profiles measured by reflectometry.

The impact of the second derivative of the density profile on the residual stress and the intrinsic flow gradient identified in these global nonlinear simulations might provide an explanation of the observed experimental relationship between the toroidal rotation gradient and the density logarithmic gradient [6], assuming that the latter is correlated with the second derivative of the same profile (which is much more difficult to precisely measure).

References

[1] A.G. Peeters et al 2011 *Nucl. Fusion* **51** 094027
[2] R.M. McDermott *et al* 2014 *Nucl. Fusion* **54** 043009
[3] W.A. Hornsby *et al* 2017 *Nuclear Fusion* **57** 046008
[4] P Manas *et al*, 2017 *Plasma Phys. Control. Fusion* **59** 035002
[5] A.G. Peeters *et al* 2009, *Computer Physics Communications* **180** 2650
[6] C. Angioni *et al* 2011, *Phys. Rev. Lett.* **107** 215003